Published in final edited form as:
Hear Res. 2013 October ; 304: 41–48. doi:10.1016/j.heares.2013.06.003.

A new *Atp2b2* deafwaddler allele, *dfw*^{i5}, interacts strongly with *Cdh23* and other auditory modifiers

Claire J. Watson[a] and **Bruce L Tempel**[a,b]

[a]The Virginia Merrill Bloedel Hearing Research Center, Department of Otolaryngology-Head and Neck Surgery, University of Washington, Box 357923, Seattle, WA 98195, USA

[b]Department of Pharmacology, The Virginia Merrill Bloedel Hearing Research Center, University of Washington, Box 357923, Seattle, WA 98195, USA

Abstract

Tight regulation of calcium (Ca^{2+}) concentrations in the stereocilia bundles of auditory hair cells of the inner ear is critical to normal auditory transduction. The plasma membrane Ca^{2+} ATPase 2 (PMCA2), encoded by the *Atp2b2* gene, is the primary mechanism for clearance of Ca^{2+} from auditory stereocilia, keeping intracellular levels low, and also contributes to maintaining adequate levels of extracellular Ca^{2+} in the endolymph. This study characterizes a novel null *Atp2b2* allele, *dfw*^{i5}, by examining cochlear anatomy, vestibular function and auditory physiology in mutant mice. Loss of auditory function in PMCA2 mutants can be attributed to dysregulation of intracellular Ca^{2+} inside the stereocilia bundles. However, extracellular Ca^{2+} ions surrounding the stereocilia are also required for rigidity of cadherin 23, a component of the stereocilia tip-link encoded by the *Cdh23* gene. This study further resolves the interaction between *Atp2b2* and *Cdh23* in a gene dosage and frequency-dependent manner, and finds that low frequencies are significantly affected by the interaction. In +/*dfw*^{i5} mice, one mutant copy of *Cdh23* is sufficient to cause broad frequency hearing impairment. Additionally, we report another modifying interaction with *Atp2b2* on auditory sensitivity, possibly caused by an unidentified hearing loss gene in mice.

Keywords

PMCA2; *Atp2b2*; mouse; *ahl*; genetic modifier; deafwaddler

1. Introduction

Calcium (Ca^{2+}) is a critical electrochemical charge carrier as well as second messenger. The concentration of Ca^{2+} in the cytoplasm needs to be maintained at a low level to permit Ca^{2+} flux into the cell upon channel opening. Low cytosolic levels also allow cells to be sensitive to small changes in Ca^{2+} concentration and favor its use as a signaling molecule. Conversely, high concentrations of intracellular Ca^{2+} can induce cytotoxicity and subsequent cellular death. Removal of Ca^{2+} following cell activity in addition to

Contact Information: Correspondence should be sent to: Bruce Tempel, Virginia Merrill Bloedel Hearing Research Center, University of Washington, Box 357923, Seattle, WA 98195, USA (bltempel@uw.edu) (Phone: 1-206-616-4693).

maintenance of low intracellular concentrations occurs via several mechanisms that include endogenous Ca^{2+} buffers, extrusion into extracellular space and incorporation of Ca^{2+} into intracellular compartments (Beurg et al., 2010; Carafoli, 2002; Clapham, 2007; Mammano et al., 2007). Members of the plasma membrane Ca^{2+} ATPase (PMCA) family are responsible for pumping Ca^{2+} from the cytoplasm across the plasma membrane, and into extracellular space by utilizing energy from ATP.

The second isoform of this family, PMCA2, is encoded by the *Atp2b2* gene and is widely expressed in the mammalian central nervous system (Stauffer et al., 1995). PMCA2 is one of the most efficient PMCA isoforms (Brini et al., 2003) and can pump effectively even in the absence of calmodulin (Hilfiker et al., 1994; Schultz et al., 2005). One of the most important contributions of PMCA2 to normal mammalian physiology is its role in the inner ear. PMCA2 is expressed in the stereocilia bundles of both auditory and vestibular hair cells, in addition to the spiral ganglion neurons that innervate these cells (Dumont et al., 2001; Furuta et al., 1998; Kozel et al., 1998; McCullough et al., 2007; Street et al., 1998; Wood et al., 2004; Yamoah et al., 1998). The hair cells of the organ of Corti are highly dependent on PMCA2 activity. During mechanotransduction in auditory hair cells, Ca^{2+} enters through the mechanoelectric transducer (MET) channels at the tips of the stereocilia and must be removed quickly for continuous auditory transduction. MET channels are cation selective and currents are primarily carried by K^+ and Ca^{2+} ions (Corey et al., 1979; Ohmori, 1987). In addition to carrying part of the conduction charge, Ca^{2+} is also essential for slow and fast adaptation in the stereocilia (Eatock, 2000; Fettiplace et al., 2003), allowing these cells to respond to sustained stimuli.

Several mouse mutants have confirmed the dependence of auditory transduction on PMCA2 (Bortolozzi et al., 2010; Dumont et al., 2001; Kozel et al., 1998; McCullough et al., 2004; Spiden et al., 2008; Street et al., 1998; Takahashi et al., 1999; Yamoah et al., 1998). In addition to mouse models, PMCA2 dysfunction can also contribute to hearing loss in humans (Ficarella et al., 2007; McCullough et al., 2007; Schultz et al., 2005). Polymorphisms in the *ATP2B2* gene can exacerbate human hearing loss when expressed in conjunction with another mutated gene (Ficarella et al., 2007; Schultz et al., 2005). Of note, one of the known human genes modified by *ATP2B2* is *CDH23*. The mouse homolog, *Cdh23*, is also known modifier of *Atp2b2* (Noben-Trauth et al., 2003). The interaction between the $Cdh23^{ahl}$ allele (herein referred to as *ahl*), has been reported in $+/dfw^{2J}$ mice that are also homozygous for *ahl* and has been largely qualitative in nature. Due to the direct correlate to human hearing loss, a higher resolution analysis of the interaction in mouse is warranted.

In addition to auditory hair cells, PMCA2 has been shown to be expressed in the vestibular sensory epithelia of the inner ear, as well as in the Purkinje neurons of the cerebellum (Burette et al., 2003; Empson et al., 2007; Stauffer et al., 1995; Street et al., 1998; Wood et al., 2004). Accordingly, PMCA2 mutants also display vestibular and motor phenotypes that can range from mild to very severe (Bortolozzi et al., 2010; Kozel et al., 1998; McCullough et al., 2004; Spiden et al., 2008; Street et al., 1998; Takahashi et al., 1999). Mice with null *Atp2b2* alleles have an unsteady gait and difficulty remaining upright even at rest (Kozel et al., 1998; McCullough et al., 2004; Street et al., 1998). In the saccule of the inner ear, PMCA2 knockout mice have been shown to lack otoconia (Kozel et al., 1998). Conversely, morphological differences in the overall cellular structure of the cerebellum of PMCA2 null mice reported to date have been minor (Empson et al., 2010; Kozel et al., 1998), although Purkinje neurons themselves have stunted dendrites (Empson et al., 2007) and sub-cellular changes in molecular composition have also been reported (Kurnellas et al., 2007). In this study, we set out to characterize the vestibular, anatomical and auditory phenotype of a

novel PMCA2 mutant, *dfw*^{i5}, while also examining the modifier effect of the *ahl* allele in a gene dosage dependent manner, and across a range of frequencies.

2. Materials and Methods

2.1. Animals

Three strains of deafwaddler mice were used in this study. The *Atp2b2*^{dfwi5} allele arose in a mutagenesis screen wherein DBA/2J mice were exposed to N-ethyl-N-nitrosourea (ENU) then crossed to C57BL/6J and screened for motor disorders at the Ernest Gallo Clinic and Research Center (Speca et al., 2006). Originally identified as Line 70, the mutant was transported from San Francisco to the Tempel Lab, transferred into the good-hearing CBA/CaJ background, and (in recognition of the route traveled) renamed *dfw*^{i5} (kind gift of A. Peterson). Mice used for auditory characterization were from a range of generations as described at length in sections 3.4 and 3.5. Mice used for rotarod and swim tests were from N3-N5, and those used for scanning electron microscopy were from N6. The *Atp2b2*^{dfw} allele arose spontaneously in C3H/HeJ mice and was obtained by our lab in 1989 from The Jackson Lab (JAX). The *Atp2b2*^{dfw2J} allele arose spontaneously in CBy.A/J-*Ttc7*^{fsn} at JAX and was obtained in 1997. Both strains have been backcrossed to good hearing CBA/CaJ for more than 20 generations in the Tempel Lab resulting in the congenic strains CBACa.C3-*Atp2b2*^{dfw} (referred to here as *dfw*) and CBACa.Cby-*Atp2b2*^{dfw2J} (referred to as *dfw*^{2J}). All strains are maintained in a backcross to CBA/CaJ obtained from JAX and replaced every 3-4 generations to retain a stock that is isogenic with CBA/CaJ at JAX. Animals were maintained on a 12 hour light/dark cycle and kept in an environment with minimal exposure to noise. All procedures were approved by the University of Washington Institutional Animal Care and Use Committee.

2.2. Auditory Testing

All mice were tested for auditory sensitivity using auditory-evoked brainstem responses (ABRs) at five weeks of age across frequencies ranging from 5.6 kHz to 40 kHz. Mice were anesthetized with a mixture of ketamine (130 mg/kg) and xylazine (10 mg/kg) prior to auditory testing and put into a sound proof box on a heating pad and secured with a bite plate. The speaker output was calibrated at the beginning of each test day. A series of 350 tones at a given frequency and intensity were administered and brain responses were recorded with two electrodes placed subcutaneously at the forebrain and hindbrain. A reference electrode was placed on the animal's hindlimb and electrocardiogram recordings were monitored to ensure an appropriate level of anesthesia throughout the experiment. Tones were 3 ms long with a 1 ms rise/fall $\cos^2$ function (delivered with alternating polarity). Brainwaves were recorded for 15 ms following the initiation of each tone with 75 ms spacing between repetitions (13.3 Hz). ABRs are amplified (1000x) and filtered (0.3-3 kHz) by a pre-amplifier (P55; Grass-Telefactor, West Warwick, RI) and digitized. Threshold at a particular frequency was determined by visual detection as the lowest intensity sound (dB SPL) which evoked a recognizable and reproducible brainwave (at least 2 out of 3 trials), usually wave V.

2.3. Behavioral/Vestibular Testing

Mice were assessed for complex motor and vestibular function between P33-P37 using rotarod tests and between P39-P43 using swim tests. For rotarod testing, mice were placed on a rod and allowed to equilibrate to the apparatus. Training sessions required that each animal tested was able to remain on a stationary rod for 30s and on a rotating rod for 90s at 5 rpm, and were given two opportunities to do so. Mice that were unable to pass training did not participate in test trials. Mice were rested for 30 minutes before testing on Day 1 and then performed six trials with an initial speed of 0.0 rpm and an acceleration speed of 0.2

rpm/s. Six more trials were performed on Day 2 using the same parameters as on Day 1. For swim testing, mice were placed into a warm (30 °C) water bath and swimming style and vigor were scored on a 3 point scale as previously reported (Kiernan et al., 1999; Marshall et al., 1979). The ability of each mouse tested to resurface after forced submersion was noted.

2.4. Expression Analysis

For all assays, tissue was collected from mice between five and six weeks of age. For protein Western blots, fresh brain tissue was flash frozen on dry ice and stored at −80 °C until further use. Tissue was equilibrated for 30 minutes at −20 °C, homogenized in cold lysis buffer (20 mM NaF, 1 mM Na vanadate, 0.5% Triton X-100, 0.1% SDS, 1xTBS pH 7.4) with 10 μL/mL protease inhibitor cocktail added immediately prior to use (Sigma). Protein concentrations of each sample were determined using a BCA assay (Pierce) and a NanoDrop Spectrophotometer ND-1000 (NanoDrop Technologies Inc.). Samples were prepared for Western blotting by diluting in an appropriate amount of lysis buffer and adding sample buffer [62.5 mM Tris-HCl pH 6.8, 5 mM EGTA, 25% glycerol, 2% SDS, 0.01% bromophenol blue, and 350 mM DTT (added fresh)] in a 1:1 ratio. Total brainstem protein (5 μg) was loaded into wells of a 4-20% gradient polyacrilamide RGEL (BioRad) for each strain and genotype and a standard Western blotting protocol using nitrocellulose membranes (BioRad) was followed. Primary antibody concentrations for β-actin (monoclonal, anti-mouse, Sigma) and PMCA2 (N-terminal, polyclonal, anti-rabbit, Affinity BioReagents) were 1:15,000 and 1:7,500 respectively. Secondary antibody concentrations against mouse and rabbit IgG respectively (GE Healthcare), were also at 1:15,000 and 1:7,500 dilutions and the ECL Plus detection reagent (GE Healthcare) was used for visualization. Western blots were visualized immediately using a Fotodyne Luminary/FX instrument (Fotodyne Inc.) with chemiluminescent detection capabilities. Quantification of protein bands was done on non-manipulated images taken using PC Image software (Fotodyne Inc.) and analyzed using ImageJ (NIH). PMCA2 expression in each lane was normalized to β-actin expression. Heterozygous and homozygous expression levels were determined as a percentage of wild-type expression for each blot. The image published in this manuscript was inverted to look like a conventional blot developed using film.

For RNA expression analysis, fresh brainstem tissue was stored in RNA*later* (Qiagen), equilibrated for 24 hours at 4 °C to allow the solution to penetrate the tissue, and transferred to −20 °C for later use. RNA was isolated using the RNeasy Plus Universal Mini Kit (Qiagen) according to the manufacturer's protocol. Homogenization was accomplished using a POLYTRON PT 1200 rotor-starter homogenizer. Total RNA from each sample (2 μg) was reverse-transcribed into complimentary DNA (cDNA) using SMARTScribe Reverse Transcriptase (Clontech) and random hexamer primers (Applied Biosystems). These samples were used for quantitative PCR (qPCR) analysis using SYBR green master mix (BioRad) and primers designed for Total-*Atp2b2* (PMCA2) as well as for reference genes *Actb* (*β*-actin) and *Sdha* (succinate dehydrogenase, subunit A). Forward and reverse primer sequences are the same as those used previously in the Tempel lab (Silverstein et al., 2006). The qPCR reactions were done on a BioRad iCycler with iQ5 software. Data for each sample is an average of at least three runs where technical replicates had a relative standard deviation (RSD) of less than 3% for each primer set.

2.5. Scanning Electron Microscopy

Scanning electron microscopy was adapted from a previously described method (Marean et al., 1995). Cochleae from 5-6 week old mice were dissected rapidly and placed in 0.1 M sodium cacodylate buffer containing 0.001% $CaCl_2$ (pH 7.4), the stapes removed and the oval window opened. A small hole was made at the apex of the cochlea, which was immediately perfused with the same buffer containing 4% glutaraldehyde by injecting

fixative into the oval window. Cochleae were incubated at room temperature on a shaker for 1 hour in 4% glutaraldehyde-containing buffer, and then stored overnight at 4 °C in fresh fixative. The next day, cochleae were washed 3 times for 10 minutes each in 0.1 M sodium cacodylate buffer (pH 7.4) and then placed in the same buffer containing 1% osmium tetroxide on a shaker for 30 minutes at 4 °C in light-protected containers. The remainder of the procedure was as previously described. After initial imaging sessions of the apical portion of each cochlea, further dissection was required to expose middle and basal portions of the epithelium. Electron micrographs were collected from a JEOL JSM-840A scanning electron microscope (JEOL Ltd.) at 20 kV equipped with a JEOL DSG Plus digital scan imaging system (JEOL Ltd.). The relative location and distance from the apex of each image was noted. Hair cells counted for apical, middle, and basal turns fall between, 0.2-1.4 mm, 1.6-3.0 mm, and 3.4-4.8 mm of a total 5.1 mm from the apex and represent an average of 473 μm, 655 μm, and 615 μm of epithelium/cochlea imaged, respectively.

2.6. Statistics

Statistical analysis was performed using Prism (GraphPad Software, Inc.). When appropriate, an ANOVA was performed followed by Bonferroni post-hoc comparisons to detect differences between strains or genotypes. A description of exact statistical measures used for each experiment is provided in the text or figure legend.

3. Results

3.1. dfw^{i5} is a PMCA2 null allele

The *dfw^{i5}* allele was identified in an ENU mutagenesis screen, sequenced, and sent to our lab for characterization (Speca et al., 2006). The *dfw^{i5}* point mutation is an A → T substitution at coding base pair 1738 in exon 12 of *Atp2b2* (Fig. 1A). The nonsense mutation predicts a stop codon in place of a lysine critical for ATP-coordination in the nucleotide binding domain of PMCA2. Two previously described deafwaddler alleles (*dfw^{2J}* and *dfw^{3J}*) encode premature stop codons and result in null PMCA2 alleles (McCullough et al., 2004; Street et al., 1998). Although *dfw^{i5}* also encodes a premature stop codon, the nature of the mutation is different (*dfw^{2J}* and *dfw^{3J}* are deletions while *dfw^{i5}* is a point mutation) making it feasible that the *dfw^{i5}* transcript is not recognized as aberrant and results in a truncated protein product. To determine the outcome of the *dfw^{i5}* mutation, Western blots using brainstem tissue from multiple mice of each genotype were assessed for PMCA2 expression and/or the presence of truncation products (Fig. 1B). The expected size of a truncation product for *dfw^{i5}* is 67 kDa and the band should appear about mid-way between PMCA2 and β-actin staining. Using an N-terminal antibody to PMCA2, no visible truncation product (nor full-length protein) was detected in *dfw^{i5}*/*dfw^{i5}* mice. The absence of a truncation product was confirmed using a variety of exposure times, antibody concentrations, total protein loading amounts and tissue types (including cochlea). Accordingly, *dfw^{i5}*, like *dfw^{2J}* and *dfw^{3J}*, appears to be a PMCA2-null allele. Reduced PMCA2 expression is also seen in +/*dfw^{i5}* mice compared to wild-type littermates (Fig. 1B).

Next, we looked to see if transcript levels were also affected by the *dfw^{i5}* mutation. Total RNA from brainstem of 5 week old mice was converted to cDNA and total *Atp2b2* transcript levels were quantified by real-time PCR. Expression was the highest in wild-type controls, reduced in +/*dfw^{i5}* and minimal in *dfw^{i5}*/*dfw^{i5}* (Fig. 1C). The reduction of expression in mutant animals is notable considering that the primary transcript of *dfw^{i5}* is only one nucleotide different than the wild-type transcript. Additionally, the secondary structure (Hofacker, 2003) of the *dfw^{i5}* transcript is predicted to be as stable as the wild-type transcript (Supplemental Fig. 1). This suggests that processing of the 296 kb long primary transcript is tightly regulated to ensure the integrity of the mature, 7 kb *Atp2b2* transcript.

3.2. Vestibular dysfunction is evident in dfw^{i5}/dfw^{i5} but not in +/dfw^{i5} mice

Mice containing mutations in *Atp2b2* are reported to display both auditory and vestibular deficits. To assess the degree to which the *dfw^{i5}* allele affects vestibular function, these mice were compared to the previously described *dfw* and *dfw^{2J}* alleles. Biochemical assays have estimated that the *dfw* mutation reduces Ca^{2+} transport by PMCA2 to 30% (Penheiter et al., 2001), while the *dfw^{2J}* allele presumably confers no Ca^{2+} ATPase activity (McCullough et al., 2004). Homozygous mutants for *dfw* and *dfw^{2J}* alleles have an obvious vestibular phenotype, with that of *dfw^{2J}*/*dfw^{2J}* being the most severe.

Homozygous *dfw^{i5}* mutant animals also have a profound balance defect similar to that of *dfw^{2J}*/*dfw^{2J}*. The *dfw^{i5}* mutants showed difficulty remaining upright, circling and head-tossing. The *dfw^{i5}*/*dfw^{i5}* mutant mice could not remain on a stationary rod nor were they able to stay afloat after being placed in a water bath, and thus, did not qualify for testing by passing the training criteria in either the rotarod or swim tasks (Fig. 2A). Homozygous *dfw^{2J}* mice also performed poorly in a swim test where they were unable to stay afloat for even a few seconds (data not shown). However, heterozygous mice for each strain were able to perform equally well as wild-type littermates in both rotarod (Fig. 2B) and swim (Fig. 2C) tests. This differs from previously published data indicating that +/*dfw^{2J}* animals had a shorter latency to fall when compared to wild-type littermates in a rotarod test (McCullough et al., 2004). The disparity between these results may be due to the age at which the mice were tested. Mice tested in this study were P33.4 ± 0.5 and P33.5 ± 0.5 for wild-type and heterozygous individuals, respectively, while mice tested previously were younger (about 7 days) and lighter (at least 2 grams on average). It is possible that younger mice may not be able to compensate for a vestibular deficiency or that this behavioral phenotype is more apparent at an earlier developmental stage. Additionally, the ability to remain on the rotating rod may be affected by the weight and size of the animal being tested.

3.3. Abnormal stereocilia bundles indicate hair cell loss in dfw^{i5} mutants

To examine anatomical abnormalities in the auditory sensory epithelium resulting from the *dfw^{i5}* allele, scanning electron microscopy was performed on whole cochlea from 5-6 week old +/+, +/*dfw^{i5}* and *dfw^{i5}*/*dfw^{i5}* mice (Fig. 3). Images shown are representative of the apex, middle and basal cochlear turns for each genotype unless otherwise noted. Wild-type cochleae displayed organized stereocilia bundles of both inner and outer hair cells (IHCs and OHCs, respectively) throughout the organ of Corti (Fig. 3A, E and I). The +/*dfw^{i5}* mice had stereocilia bundles ranging from generally normal (albeit slightly compressed) to disorganized and fused stereocilia (Fig. 3B, F and J). The *dfw^{i5}*/*dfw^{i5}* cochleae contained disorganized, dysmorphic (fused and often stubby) stereocilia bundles that appeared more abnormal towards the basal, high frequency area of the cochlea (Fig. 3C, G and K). Moreover, missing stereocilia bundles (indicating dead or missing hair cells) were virtually non-existent in wild-type cochlea while the frequency of missing stereocilia bundles was quite dramatic in regions of *dfw^{i5}*/*dfw^{i5}* cochleae, especially in the base where bundles were sparsely distributed if present at all. A patch of stereocilia bundles is shown for the base of *dfw^{i5}*/*dfw^{i5}* (Fig. 3K) to reflect the abnormal morphology, although this is not representative of the number of hair cells at this location in the cochlea (see Fig. 3L). Cochleae of +/*dfw^{i5}* mice showed an intermediate phenotype with occasional missing stereocilia bundles in the apex and middle cochlear turns and increasing loss towards the base (Fig. 3D, H and L). A one-way ANOVA between genotypes for each cell type (IHC or OHC) indicated a significant effect of genotype for apical, middle and basal IHCs ($p < 0.0005$, $p < 0.003$ and $p < 0.0001$, respectively), as well as OHCs of the middle and basal turns ($p < 0.05$ and $p < 0.002$, respectively). Bonferroni post-hoc comparisons showed significant differences between genotypes indicated in Fig. 3D, H and L. It is important to note that cells with abnormal stereocilia were counted despite the negative effect this would likely have on

auditory transduction. Therefore, the averages presented should be considered a conservative estimate of functional loss. Additionally, smaller bundles (which may not function normally) were frequently seen in the middle and base of +/*dfw*^{i5} cochleae; these may contribute to the increased OHC density in the middle turn, IHC density in the basal turn, and to the increased variability in OHC counts in the basal turn of the cochlea for this genotype (Fig. 3H and L).

3.4. The dfw^{i5} allele interacts strongly with the ahl locus

The *dfw*^{i5} mutation was induced by chemical mutagenesis in DBA/2J and was identified in a mouse with mixed DBA/2J and C57BL/6J genetic background (see Methods, "*Animals*"). Since null *Atp2b2* mutants are completely deaf (data not shown), auditory sensitivity was assessed in +/*dfw*^{i5} mice after transferring the *dfw*^{i5} allele into the good-hearing CBA/CaJ background. We began to monitor auditory sensitivity in +/*dfw*^{i5} starting in the third generation (N3) and noticed a large degree of variability in ABR at 8, 11.3 and 16 kHz in these individuals. The original age-related hearing loss locus (*ahl*) is present in both the DBA/2J and C57BL/6J ancestral strains so the *Cdh23*^{G753A} single-nucleotide polymorphism (SNP) associated with this locus was used to screen for the presence of an *ahl* modifier allele in our line.

The *Cdh23*^{753A} allele alters splicing in the *Cdh23* gene encoding cadherin 23 (Noben-Trauth et al., 2003), a structural protein required to form tip-links in the stereocilia of auditory hair cells (Kazmierczak et al., 2007; Siemens et al., 2004). The *ahl* allele has been associated with early onset age-related or progressive hearing loss in several mouse strains (Johnson et al., 2000; Zheng et al., 2001). Homozygosity at *ahl* has been shown to reduce auditory sensitivity in +/*dfw*^{2J} mice (Noben-Trauth et al., 2003; Noben-Trauth et al., 1997) and heterozygosity at *ahl* has been reported to exacerbate the already severe phenotype of the hypofunctional PMCA2 mutant, +/*Obl* (Spiden et al., 2008). However, the extent of this interaction has not been fully defined by *ahl* allele dosage, or across a broad range of frequencies.

Therefore, ABR data for +/*dfw*^{i5} mice from N3 to N5 was grouped by *Cdh23*^{G753A} genotype (Fig. 4). The *Cdh23*^{753A} allele had a strong effect on the auditory phenotype of +/*dfw*^{i5} individuals, with the most significant effect on sensitivity occurring at lower frequencies. At N3, only one mouse was homozygous at the *ahl* locus and had the most severe hearing loss of any animal (Fig. 4, closed squares). The +/*dfw*^{i5} mice that were also heterozygous for the *ahl* allele were severely affected across all frequencies (Fig. 4, half-filled squares), and those mice that were negative for the *ahl* allele (CBA-like at this locus) have significant hearing loss at mid- and high-frequencies (Fig. 4, open squares).

Notably, another locus, *ahl8*, has also been associated with early-onset hearing loss in DBA/2J. Hearing loss associated with *ahl8* is caused by a point mutation in the *Fscn2* gene (Shin et al., 2010). To check if this hearing loss locus might also contribute to the +/*dfw*^{i5} phenotype, all animals from the N3 generation which were subjected to ABR testing (a total of 12 mice) were screened for the *ahl8* SNP. The *ahl8* allele was not present in any of these mice, confirming that it was not carried into our line and does not affect the phenotype of mice used in this study.

3.5. A phenotype shift in +/dfw^{i5} suggests an interaction with a novel modifier

To fully define the extent of hearing loss in +/*dfw*^{i5}, the allele was transferred into CBA/CaJ for a total of 10 generations, where mice are estimated to retain only 0.2% of their ancestral background. However, to evaluate the stability of the auditory phenotype, sensitivity in +/*dfw*^{i5} was first assessed beginning at N3 in addition to N4, N5, N6 and N10 (Fig. 5). Only

mice negative for the *ahl* allele, which was crossed out of the line between N4 and N5, were used in this comparison. The +/*dfw*^{i5} mice in generations N3, N4 and N5 all had a similar phenotype with statistically significant hearing loss at most frequencies compared to controls and were not statistically different from one another (statistical analysis of Fig. 5 is given in Supplemental Table 1). However, a shift in sensitivity occurred in N6 where thresholds significantly improved for +/*dfw*^{i5} mice at low and mid-frequencies, with the most dramatic shifts occurring at 16 and 22.6 kHz. At N10, +/*dfw*^{i5} are not statistically different from N6, confirming that the auditory phenotype of this line was stable for several generations. Accordingly, the final auditory characterization of +/*dfw*^{i5} shows relatively similar sensitivity to other known heterozygous PMCA2 null mutants with dramatic hearing loss at high frequencies, but relatively normal thresholds at low- and mid-frequencies when tested at five weeks.

Taken together, the generational shift of the +/*dfw*^{i5} auditory phenotype suggests that an unidentified gene or modifier region may contribute to hearing loss in DBA or B6 strains, that this gene interacts with *Atp2b2*, and that it was crossed out of our line between N5 and N6. Alternatively, it is possible that another polymorphism induced by the ENU mutagenesis in DBA is interacting with *Atp2b2* to modify hearing. Since the *ahl* and *ahl8* alleles were crossed out of our line prior to N5, it is unlikely that a unique *Cdh23* or *Fscn2* allele is modifying *Atp2b2* in this cross. To our knowledge, no other identified hearing loss genes are present in these strains. To assess if the unknown locus was directly affecting regulation of PMCA2 or *Atp2b2*, protein and mRNA levels were quantified from mice in three generational groups: N3-N5 (when the modifier was present), N6 (after the shift in sensitivity) and N10 (when the modifier should no longer be present). PMCA2 expression is unchanged between the generational groups (Fig. 6A) with heterozygotes expressing 67.1%, 63.7% and 63.3% of control expression in N3-N5, N6 and N10, respectively. Similarly, there is no difference in mRNA expression between mice of each generational group with heterozygotes expressing approximately half the level of total *Atp2b2* transcript as wild-type mice (Fig. 6B). Thus, the proposed modifier function of the unknown locus does not appear to affect PMCA2 or *Atp2b2* expression directly and likely involves another gene.

4. Discussion

Here, we report and characterize a new PMCA2 null allele, *dfw*^{i5}. Similar to other null PMCA2 mutants, homozygotes are completely deaf and have a severe ataxia. Heterozygotes have impaired auditory transduction but no discernible motor or vestibular abnormalities. That an impairment on the rotarod behavioral task has been previously reported in similar null heterozygous mutants, +/*dfw*^{2J} and +/*dfw*^{3J} (McCullough et al., 2004), suggests mice haploinsufficient for PMCA2 may sit at the cusp of vestibular impairment. Presumably, these mice have approximately 50% Ca^{2+} clearance activity relative to controls and that this represents the critical amount of PMCA2 necessary for normal vestibular behavior. Just a small reduction in PMCA2 activity to 30% in *dfw*/*dfw* leaves these mice with an overt vestibular phenotype. Another step-wise decrease in PMCA2 seen in *dfw*^{i5}/*dfw*^{i5} and *dfw*^{2J}/*dfw*^{2J} animals noticeably worsens the impairment, implying that we can estimate from 0% to 50% activity as a range where PMCA2 function is physiologically important for vestibular behavior.

In contrast, the 30% activity in *dfw*/*dfw* is not sufficient for any detectible auditory brainstem responses. While responses are present in +/*dfw*^{i5}, sensitivity is still greatly affected, particularly at high-frequencies. At the highest frequencies tested, 32 and 40 kHz, +/*dfw*^{i5} mice have lost about 40-45 dB SPL in sensitivity compared to wild-type, which is equivalent to the estimated contribution of outer hair cells as the cochlear amplifier (Prosen et al., 1978; Ryan et al., 1977; Stebbins et al., 1979). Paired with the anatomical data for +/

dfw^{i5} cochleae, we can conclude that, at 5 weeks of age, many stereocilia bundles of the high-frequency hair cells at the base of the cochlea are present but are not functioning normally. This supports what has been previously reported in loss of function PMCA2 mutants (Bortolozzi et al., 2010; Spiden et al., 2008) and can be extended to null PMCA2 mutations. Studies that have examined the anatomy of *dfw*^{2J} mutants have focused only on homozygous mutants and were qualitative in nature (Street et al., 1998; Wood et al., 2004). Here we provide a quantitative measure of hair cell counts and a complete report of hair cell morphology across the entire sensory epithelium for both heterozygous and homozygous PMCA2 null mice.

The presence of stereocilia in the sensory epithelium even when transduction is greatly affected indicates that there is a lag, which may be considerable, between loss of hair cell function and complete hair cell death evidenced by loss of stereocilia bundles. Of note, relatively normal stereocilia bundles on the surface of the organ of Corti have been reported even in mice with non-functioning or abnormal hair cell bodies (Bock et al., 1983). This is also demonstrated by the presence of OHC and IHC stereocilia in homozygous mutant *dfw*^{i5}/*dfw*^{i5} cochleae, which are profoundly deaf and may never have coordinated hair cell activity. Interestingly, although none of the hair cells (from the apex to the base) in the homozygous mutant are ever thought to be functional, there is still a bias toward hair cell loss at the base of the cochlea in these mice. This has been seen in other PMCA2 mutants (Bortolozzi et al., 2010; Spiden et al., 2008) and may reflect the intrinsic properties of the OHCs at this location. Supporting this idea, OHCs at the base of the cochlea are predicted to have a higher MET channel conductance resulting in a greater influx of calcium into the stereocilia bundles (Beurg et al., 2010). Recent work suggests that the density of PMCA2 expression in the stereocilia along the tonotopic axis is unchanged (Chen et al., 2012) ruling out the possibility that increased PMCA2 activity in basal hair cells could help compensate for the additional calcium current. This would be exacerbated in PMCA2 mutant mice and hair cells at the base of the cochlea would have a higher propensity for calcium overload.

Auditory function is highly sensitive to genetic manipulation, with over 120 identified loci involved in non-syndromic hearing loss in humans (Van Camp et al., 2013). In common inbred mouse strains, there are currently eight identified age-related hearing loss loci (Johnson et al., 2006). While single mutations can result in hearing loss phenotypes, interactions between multiple genetic variants can also impair auditory sensitivity. Recent studies have shown that isolated homozygosity at the *ahl* locus in an otherwise CBA/CaJ background cannot fully recapitulate the hearing loss seen in C57BL/6J (Kane et al., 2012). This indicates that other genes contribute to hearing loss in this strain, and highlights the importance of understanding the interaction between *ahl* and *Atp2b2* with better resolution.

A closer look at the modifying interaction of *ahl* within +/*dfw*^{i5} individuals reveals that low frequency hearing in the mouse is greatly impacted by the presence of even one mutated *Cdh23* allele. Although the highest frequencies in +/*dfw*^{i5} are already severely affected, thresholds at 32 and 40 kHz do not worsen in combination with the *ahl* allele. In contrast, low frequencies are significantly elevated with each copy of the *ahl* allele, and the only mouse with both affected copies at the *ahl* locus had higher thresholds in the low- to mid-frequency range than at high frequencies. This result shows that the interaction between *Atp2b2* and *Cdh23* may be much stronger than previously appreciated, and suggests that a reduction in PMCA2 expression can be critical for transduction at low frequencies. The sensitivity of the interaction between *Atp2b2* and *Cdh23* at low frequencies may be due, in part, to the morphology of the stereocilia at this location. Low-frequency hair cells at the apex of the cochlea have long stereocilia and coordinated movements of the bundle may be particularly sensitive to changes in the structural integrity of the tip link. Similarly, in humans homozygous for a mutation in *CDH23*, only one copy of a PMCA2 mutant allele is

necessary to extend hearing loss to low frequencies (Schultz et al., 2005) suggesting that the mechanism of hearing impairment via the interaction of *ATP2B2* and *CDH23* is not species specific may affect the taller, low-frequency, stereocilia bundles significantly. Furthermore, we report a possible interaction between a new modifier allele and *Atp2b2* present in earlier generations of $+/dfw^{i5}$ mice that cannot be accounted for by an interaction with the *ahl* locus.

Supplementary Material

Refer to Web version on PubMed Central for supplementary material.

Acknowledgments

We would like to thank L. Robinson for maintaining our mouse colonies; A. Peterson, D. Speca and D. Chihara for providing us with the original "Line 70" dfw^{i5} mouse; D. Cunningham for assistance with scanning electron microscopy techniques; and V. Street for comments on the manuscript. This work was supported by grants from the NIH; RO1 DC02739 (BLT), P30 DC04661 (BLT), T32 DC005361 (CJW) and T32 DC000033 (CJW).

Abbreviations

ABR	auditory-evoked brainstem response
ahl	age-related hearing loss
ANOVA	analysis of variance
Ca^{2+}	calcium
dB	decibels
dfw	deafwaddler
ENU	N-ethyl-N-nitrosourea
HET	heterozygote
IHC	inner hair cell
JAX	Jackson Laboratory
MET	mechanoelectric transducer
MFE	minimum free energy
MUT	mutant
OHC	outer hair cell
PMCA	plasma membrane calcium ATPase
SEM	standard error of the mean
SNP	single-nucleotide polymorphism
SPL	sound pressure level
WT	wild-type

References

Beurg M, Nam JH, Chen Q, Fettiplace R. Calcium balance and mechanotransduction in rat cochlear hair cells. Journal of neurophysiology. 2010; 104:18–34. [PubMed: 20427623]

Bock GR, Steel KP. Inner ear pathology in the deafness mutant mouse. Acta Otolaryngol. 1983; 96:39–47. [PubMed: 6613551]

Bortolozzi M, Brini M, Parkinson N, Crispino G, Scimemi P, De Siati RD, Di Leva F, Parker A, Ortolano S, Arslan E, Brown SD, Carafoli E, Mammano F. The novel PMCA2 pump mutation Tommy impairs cytosolic calcium clearance in hair cells and links to deafness in mice. The Journal of biological chemistry. 2010; 285:37693–703. [PubMed: 20826782]

Brini M, Coletto L, Pierobon N, Kraev N, Guerini D, Carafoli E. A comparative functional analysis of plasma membrane Ca2+ pump isoforms in intact cells. The Journal of biological chemistry. 2003; 278:24500–8. [PubMed: 12716903]

Burette A, Rockwood JM, Strehler EE, Weinberg RJ. Isoform-specific distribution of the plasma membrane Ca2+ ATPase in the rat brain. The Journal of comparative neurology. 2003; 467:464–76. [PubMed: 14624481]

Carafoli E. Calcium signaling: a tale for all seasons. Proceedings of the National Academy of Sciences of the United States of America. 2002; 99:1115–22. [PubMed: 11830654]

Chen Q, Mahendrasingam S, Tickle JA, Hackney CM, Furness DN, Fettiplace R. The development, distribution and density of the plasma membrane calcium ATPase 2 calcium pump in rat cochlear hair cells. The European journal of neuroscience. 2012; 36:2302–10. [PubMed: 22672315]

Clapham DE. Calcium signaling. Cell. 2007; 131:1047–58. [PubMed: 18083096]

Corey DP, Hudspeth AJ. Ionic basis of the receptor potential in a vertebrate hair cell. Nature. 1979; 281:675–7. [PubMed: 45121]

Dumont RA, Lins U, Filoteo AG, Penniston JT, Kachar B, Gillespie PG. Plasma membrane Ca2+-ATPase isoform 2a is the PMCA of hair bundles. The Journal of neuroscience: the official journal of the Society for Neuroscience. 2001; 21:5066–78. [PubMed: 11438582]

Eatock RA. Adaptation in hair cells. Annual review of neuroscience. 2000; 23:285–314.

Empson RM, Garside ML, Knopfel T. Plasma membrane Ca2+ ATPase 2 contributes to short-term synapse plasticity at the parallel fiber to Purkinje neuron synapse. The Journal of neuroscience: the official journal of the Society for Neuroscience. 2007; 27:3753–8. [PubMed: 17409239]

Empson RM, Turner PR, Nagaraja RY, Beesley PW, Knopfel T. Reduced expression of the Ca(2+) transporter protein PMCA2 slows Ca(2+) dynamics in mouse cerebellar Purkinje neurones and alters the precision of motor coordination. The Journal of physiology. 2010; 588:907–22. [PubMed: 20083513]

Fettiplace R, Ricci AJ. Adaptation in auditory hair cells. Current opinion in neurobiology. 2003; 13:446–51. [PubMed: 12965292]

Ficarella R, Di Leva F, Bortolozzi M, Ortolano S, Donaudy F, Petrillo M, Melchionda S, Lelli A, Domi T, Fedrizzi L, Lim D, Shull GE, Gasparini P, Brini M, Mammano F, Carafoli E. A functional study of plasma-membrane calcium-pump isoform 2 mutants causing digenic deafness. Proc Natl Acad Sci U S A. 2007; 104:1516–21. [PubMed: 17234811]

Furuta H, Luo L, Hepler K, Ryan AF. Evidence for differential regulation of calcium by outer versus inner hair cells: plasma membrane Ca-ATPase gene expression. Hearing research. 1998; 123:10–26. [PubMed: 9745951]

Hilfiker H, Guerini D, Carafoli E. Cloning and expression of isoform 2 of the human plasma membrane Ca2+ ATPase. Functional properties of the enzyme and its splicing products. J Biol Chem. 1994; 269:26178–83. [PubMed: 7929331]

Hofacker IL. Vienna RNA secondary structure server. Nucleic Acids Research. 2003; 31:3429–3431. [PubMed: 12824340]

Johnson KR, Zheng QY, Erway LC. A major gene affecting age-related hearing loss is common to at least ten inbred strains of mice. Genomics. 2000; 70:171–80. [PubMed: 11112345]

Johnson KR, Zheng QY, Noben-Trauth K. Strain background effects and genetic modifiers of hearing in mice. Brain research. 2006; 1091:79–88. [PubMed: 16579977]

Kane KL, Longo-Guess CM, Gagnon LH, Ding D, Salvi RJ, Johnson KR. Genetic background effects on age-related hearing loss associated with Cdh23 variants in mice. Hearing research. 2012; 283:80–8. [PubMed: 22138310]

Kazmierczak P, Sakaguchi H, Tokita J, Wilson-Kubalek EM, Milligan RA, Muller U, Kachar B. Cadherin 23 and protocadherin 15 interact to form tip-link filaments in sensory hair cells. Nature. 2007; 449:87–91. [PubMed: 17805295]

Kiernan AE, Zalzman M, Fuchs H, Hrabe de Angelis M, Balling R, Steel KP, Avraham KB. Tailchaser (Tlc): a new mouse mutation affecting hair bundle differentiation and hair cell survival. Journal of neurocytology. 1999; 28:969–85. [PubMed: 10900098]

Kozel PJ, Friedman RA, Erway LC, Yamoah EN, Liu LH, Riddle T, Duffy JJ, Doetschman T, Miller ML, Cardell EL, Shull GE. Balance and hearing deficits in mice with a null mutation in the gene encoding plasma membrane Ca2+-ATPase isoform 2. The Journal of biological chemistry. 1998; 273:18693–6. [PubMed: 9668038]

Kurnellas MP, Lee AK, Li H, Deng L, Ehrlich DJ, Elkabes S. Molecular alterations in the cerebellum of the plasma membrane calcium ATPase 2 (PMCA2)-null mouse indicate abnormalities in Purkinje neurons. Molecular and cellular neurosciences. 2007; 34:178–88. [PubMed: 17150372]

Mammano F, Bortolozzi M, Ortolano S, Anselmi F. Ca2+ signaling in the inner ear. Physiology. 2007; 22:131–44. [PubMed: 17420304]

Marean GC, Cunningham D, Burt JM, Beecher MD, Rubel EW. Regenerated hair cells in the European starling: are they more resistant to kanamycin ototoxicity than original hair cells? Hear Res. 1995; 82:267–76. [PubMed: 7775291]

Marshall JF, Berrios N. Movement disorders of aged rats: reversal by dopamine receptor stimulation. Science. 1979; 206:477–9. [PubMed: 504992]

McCullough BJ, Tempel BL. Haplo-insufficiency revealed in deafwaddler mice when tested for hearing loss and ataxia. Hearing research. 2004; 195:90–102. [PubMed: 15350283]

McCullough BJ, Adams JC, Shilling DJ, Feeney MP, Sie KC, Tempel BL. 3p--syndrome defines a hearing loss locus in 3p25.3. Hearing research. 2007; 224:51–60. [PubMed: 17208398]

Noben-Trauth K, Zheng QY, Johnson KR. Association of cadherin 23 with polygenic inheritance and genetic modification of sensorineural hearing loss. Nature genetics. 2003; 35:21–3. [PubMed: 12910270]

Noben-Trauth K, Zheng QY, Johnson KR, Nishina PM. mdfw: a deafness susceptibility locus that interacts with deaf waddler (dfw). Genomics. 1997; 44:266–72. [PubMed: 9325047]

Ohmori H. Gating properties of the mechano-electrical transducer channel in the dissociated vestibular hair cell of the chick. The Journal of physiology. 1987; 387:589–609. [PubMed: 3656183]

Penheiter AR, Filoteo AG, Croy CL, Penniston JT. Characterization of the deafwaddler mutant of the rat plasma membrane calcium-ATPase 2. Hearing research. 2001; 162:19–28. [PubMed: 11707348]

Prosen CA, Petersen MR, Moody DB, Stebbins WC, Hawkins JE Jr. Permanent threshold shift and cochlear hair cell loss in the kanamycin-treated guinea pig. Otolaryngology. 1978; 86:ORL-886-7.

Ryan A, McGee TJ. Development of hearing loss in kanamycin treated chinchillas. The Annals of otology, rhinology, and laryngology. 1977; 86:176–82.

Schultz JM, Yang Y, Caride AJ, Filoteo AG, Penheiter AR, Lagziel A, Morell RJ, Mohiddin SA, Fananapazir L, Madeo AC, Penniston JT, Griffith AJ. Modification of human hearing loss by plasma-membrane calcium pump PMCA2. N Engl J Med. 2005; 352:1557–64. [PubMed: 15829536]

Shin JB, Longo-Guess CM, Gagnon LH, Saylor KW, Dumont RA, Spinelli KJ, Pagana JM, Wilmarth PA, David LL, Gillespie PG, Johnson KR. The R109H variant of fascin-2, a developmentally regulated actin crosslinker in hair-cell stereocilia, underlies early-onset hearing loss of DBA/2J mice. The Journal of neuroscience: the official journal of the Society for Neuroscience. 2010; 30:9683–94. [PubMed: 20660251]

Siemens J, Lillo C, Dumont RA, Reynolds A, Williams DS, Gillespie PG, Muller U. Cadherin 23 is a component of the tip link in hair-cell stereocilia. Nature. 2004; 428:950–5. [PubMed: 15057245]

Silverstein RS, Tempel BL. Atp2b2, encoding plasma membrane Ca2+-ATPase type 2, (PMCA2) exhibits tissue-specific first exon usage in hair cells, neurons, and mammary glands of mice. Neuroscience. 2006; 141:245–57. [PubMed: 16675132]

Speca DJ, Rabbee N, Chihara D, Speed TP, Peterson AS. A genetic screen for behavioral mutations that perturb dopaminergic homeostasis in mice. Genes, brain, and behavior. 2006; 5:19–28.

Spiden SL, Bortolozzi M, Di Leva F, de Angelis MH, Fuchs H, Lim D, Ortolano S, Ingham NJ, Brini M, Carafoli E, Mammano F, Steel KP. The novel mouse mutation Oblivion inactivates the

PMCA2 pump and causes progressive hearing loss. PLoS genetics. 2008; 4:e1000238. [PubMed: 18974863]

Stauffer TP, Guerini D, Carafoli E. Tissue distribution of the four gene products of the plasma membrane Ca2+ pump. A study using specific antibodies. The Journal of biological chemistry. 1995; 270:12184–90. [PubMed: 7538133]

Stebbins WC, Hawkins JE Jr. Johnson LG, Moody DB. Hearing thresholds with outer and inner hair cell loss. American journal of otolaryngology. 1979; 1:15–27. [PubMed: 95382]

Street VA, McKee-Johnson JW, Fonseca RC, Tempel BL, Noben-Trauth K. Mutations in a plasma membrane Ca2+-ATPase gene cause deafness in deafwaddler mice. Nature genetics. 1998; 19:390–4. [PubMed: 9697703]

Takahashi K, Kitamura K. A point mutation in a plasma membrane Ca(2+)-ATPase gene causes deafness in Wriggle Mouse Sagami. Biochemical and biophysical research communications. 1999; 261:773–8. [PubMed: 10441500]

Van Camp G, Smith RJH. Hereditary Hearing Loss Homepage. 2013 [Online] http://hereditaryhearingloss.org (updated May 15th, 2013; verified May, 2013).

Wood JD, Muchinsky SJ, Filoteo AG, Penniston JT, Tempel BL. Low endolymph calcium concentrations in deafwaddler2J mice suggest that PMCA2 contributes to endolymph calcium maintenance. Journal of the Association for Research in Otolaryngology: JARO. 2004; 5:99–110. [PubMed: 15357414]

Yamoah EN, Lumpkin EA, Dumont RA, Smith PJ, Hudspeth AJ, Gillespie PG. Plasma membrane Ca2+-ATPase extrudes Ca2+ from hair cell stereocilia. The Journal of neuroscience: the official journal of the Society for Neuroscience. 1998; 18:610–24. [PubMed: 9425003]

Zheng QY, Johnson KR. Hearing loss associated with the modifier of deaf waddler (mdfw) locus corresponds with age-related hearing loss in 12 inbred strains of mice. Hearing research. 2001; 154:45–53. [PubMed: 11423214]

Highlights

1. We characterize a new *Atp2b2* null deafwaddler allele, *dfw*^{i5}.
2. Mice lacking PMCA2 have abnormal stereocilia morphology.
3. *Atp2b2* and *Cdh23* interact strongly to cause broad frequency hearing loss.
4. A second locus interacts with *Atp2b2* and modifies hearing loss in +/*dfw*^{i5}.

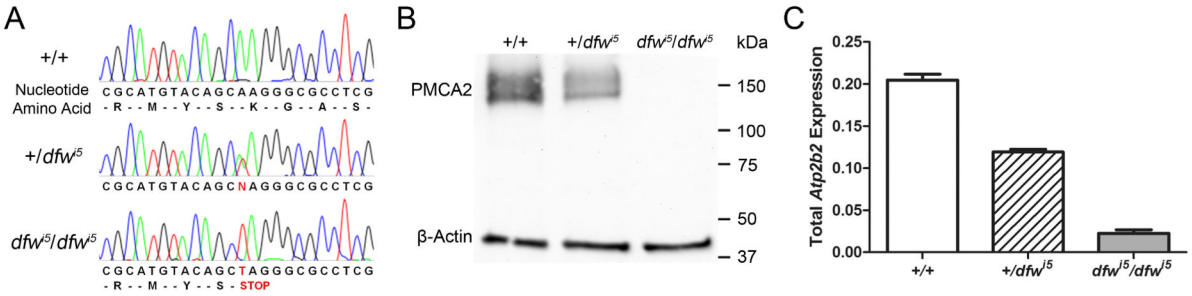

Fig. 1.

Characterization of the *dfw*^{j5} allele. (A) Electropherogram of genomic sequence from wild-type (top) as well as heterozygous (middle) and homozygous (bottom) *dfw*^{j5} mutants showing the A to T point mutation resulting in a premature stop codon. (B) A representative western blot using an N-terminal antibody to PMCA2 shows reduced expression in +/*dfw*^{j5} and no detectible expression in *dfw*^{j5}/*dfw*^{j5} mice. (C) Total RNA expression is also decreased significantly in +/*dfw*^{j5} and *dfw*^{j5}/*dfw*^{j5} mice. Error bars represent SEM.

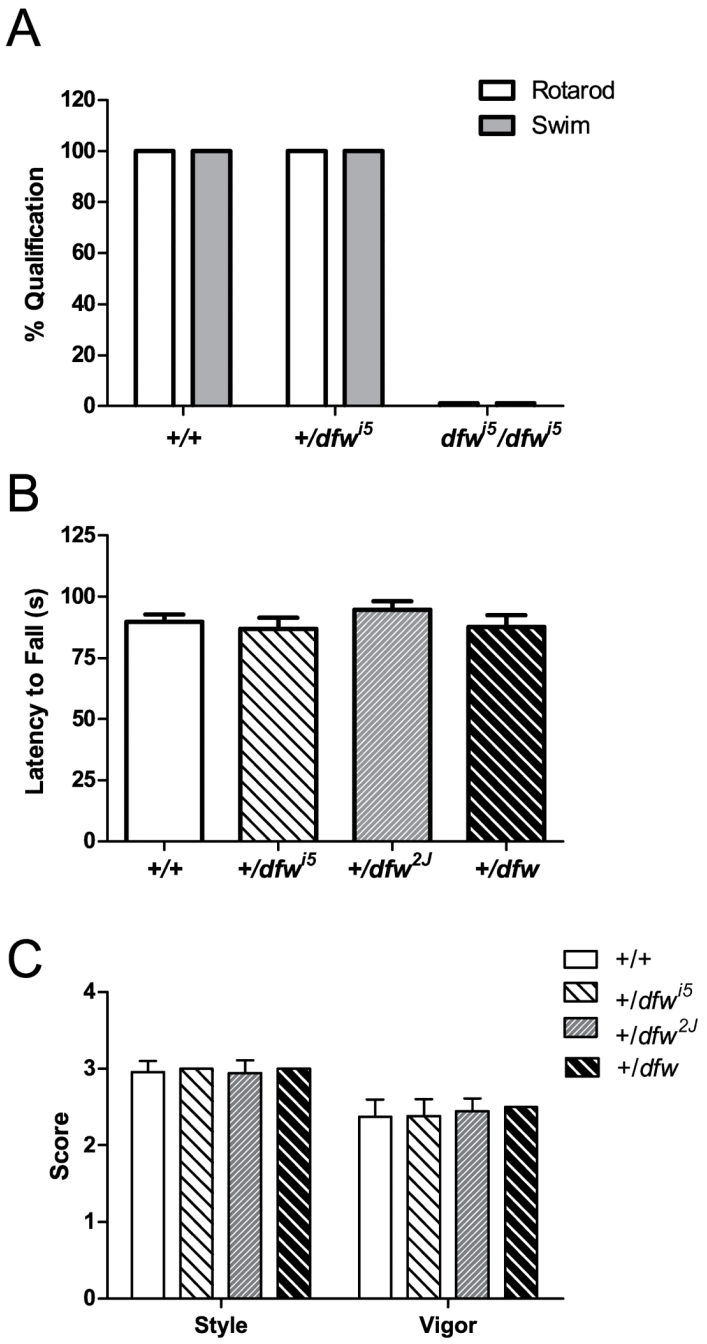

Fig. 2.

Mice heterozygous for deafwaddler alleles perform equally well as wild-type in rotarod and swim tests. (A) Percentage of mice of each genotype that passed training criteria for rotarod (open bars) and swim (gray bars) tests. All of the wild-type and +/dfw^{j5} mice passed qualification while none of the dfw^{j5}/dfw^{j5} mice could be tested. (B) Average latency to fall in rotarod tests are shown for grouped wild-type littermates (open bar) and each heterozygous deafwaddler strain (hashed bars). (C) Each mouse was assessed for their ability to swim by scoring for swimming style and vigor on a 3-point scale (see methods). Error bars represent SEM.

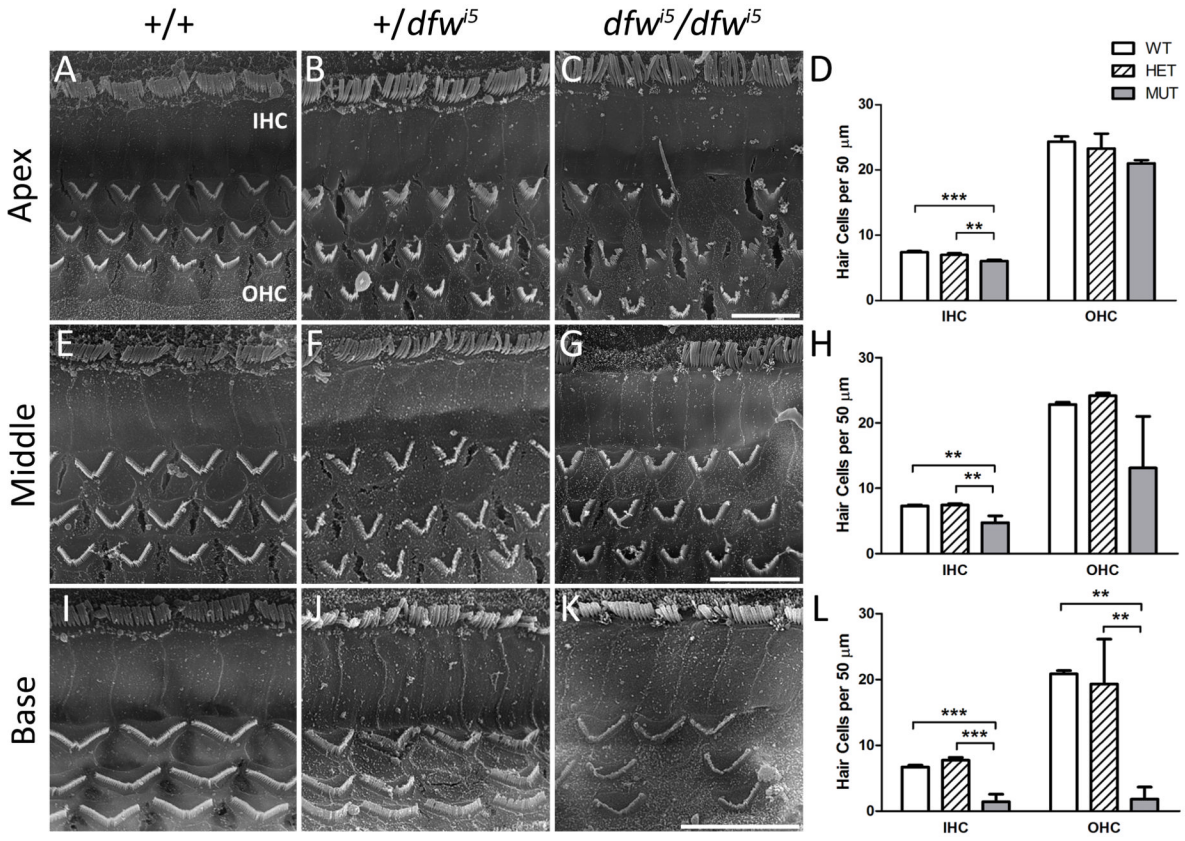

Fig. 3.

Scanning electron microscopy of *dfw*^{i5} animals. Representative images of inner (IHC) and outer hair cells (OHC) are shown for apical (A-C) middle (E-G) and basal (I-K) regions of the cochlea. Wild-type hair cells (A,E,I) are highly organized, +/*dfw*^{i5} hair cells (B,F,J) are occasionally disorganized or abnormal while *dfw*^{i5}/*dfw*^{i5} hair cells (C,G,K) are often disorganized, fused, stubby or missing. The image shown for the base of *dfw*^{i5}/*dfw*^{i5} is not representative of hair cell number, and a patch of stereocilia was chosen to reflect the morphology of mutant hair cells at this location. Scale bars = 10 µm for each row. (D,H,L) Cell counts for apical (D), middle (H) and basal (L) cochlear regions for outer and inner hair cells (n=3 for each genotype). Cells were counted if any portion of the stereocilia bundle was present despite its shape or organization. Very minimal loss was seen in hair cell counts at the apex in mutant mice. Loss was more dramatic in the middle turn of *dfw*^{i5}/*dfw*^{i5} and was progressively dramatic at the base with large regions of missing hair cells. In the base of +/*dfw*^{i5}, hair cell loss was variable with some cochleae missing a significant percentage of cells and others mostly intact (reflected by the large error bars). **p<0.01, ***p<0.001 in a Bonferroni post-hoc comparison following a one-way ANOVA. Error bars represent standard deviation.

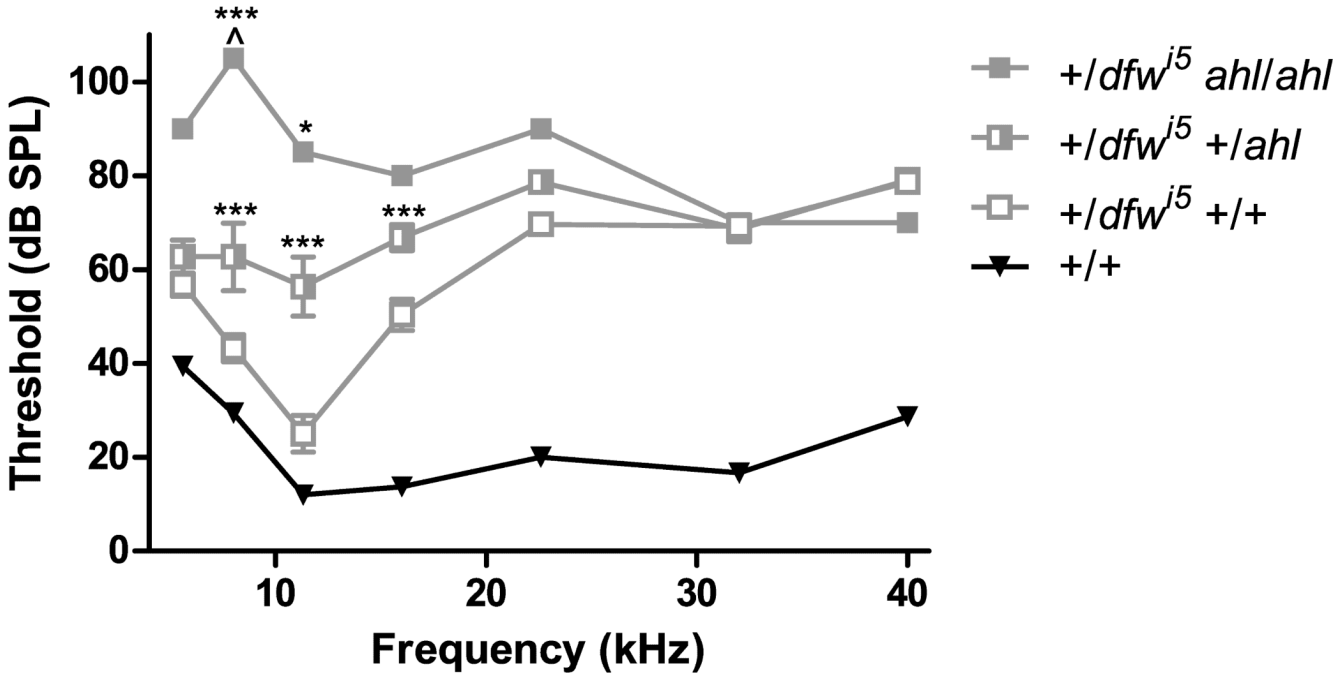

Fig. 4.

The *dfw*^{j5} allele strongly interacts with the *ahl* locus. Variability of ABR thresholds in early generations of +/*dfw*^{j5} mice segregates with the presence of the *Cdh23*^{753A} allele at the *ahl* locus. Mice negative for the *Cdh23*^{753A} allele had the best sensitivity of +/*dfw*^{j5} animals (open squares, n=14), while +/*dfw*^{j5} mice also heterozygous for the *Cdh23*^{753A} allele have increased thresholds (half-filled squares, n=11) and one +/*dfw*^{j5} mouse homozygous for the *Cdh23*^{753A} allele had severely elevated thresholds (filled squares, n=1). Average thresholds of wild-type littermates (black inverted triangles) are shown for reference. ^ Indicates no threshold was detectable at this frequency; statistics were calculated for this point as if the threshold was the highest presented intensity. Error bars represent SEM. *p<0.05 and ***p<0.001 in a Bonferroni post-hoc test following a two-way ANOVA relative to +/*dfw*^{j5} animals with one less copy of the *Cdh23*^{753A} allele.

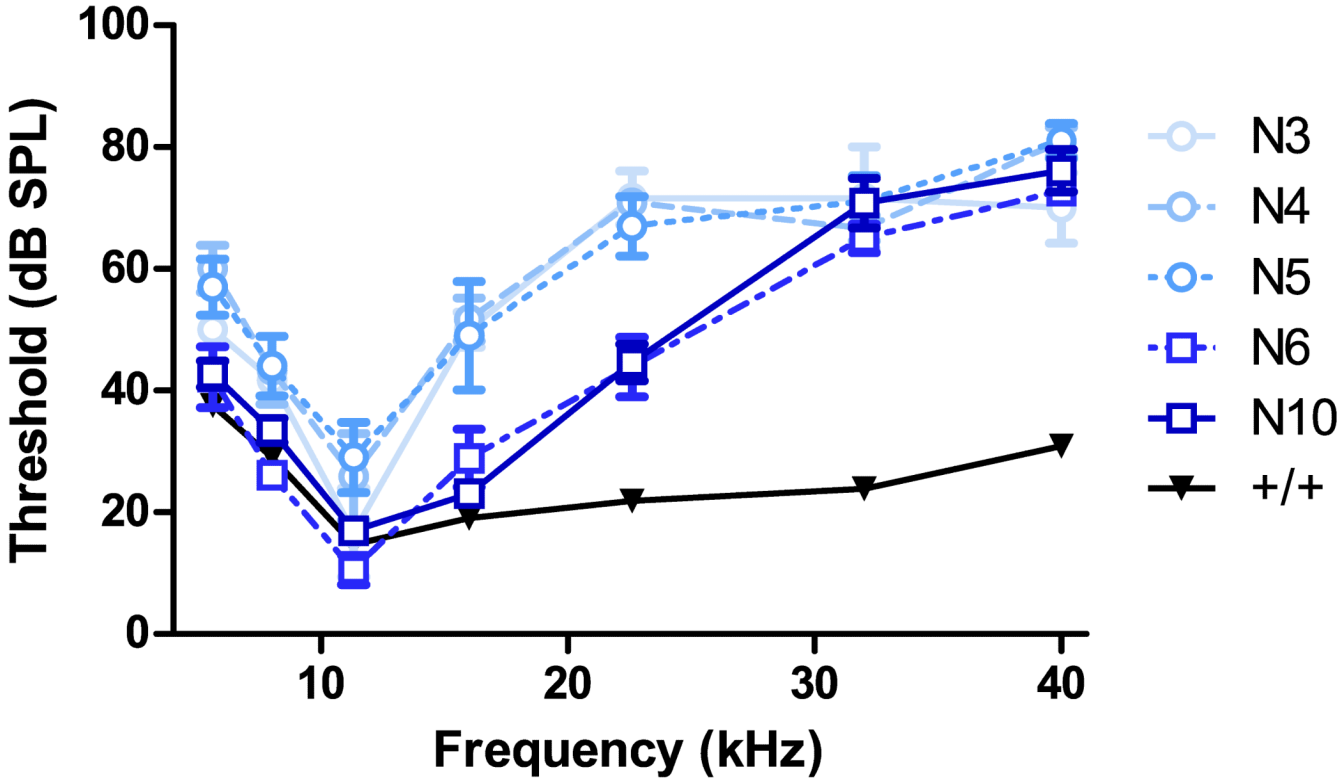

Fig. 5.

Auditory phenotype of +/*dfw*^{i5} by backcross generation. Auditory sensitivity of +/*dfw*^{i5} individuals in N3 (open circles, solid line, n = 3), N4 (open circles, large dashed line, n = 6) and N5 (open circles, small dashed line, n = 5) was similar. A shift in phenotype occurred at N6 (open squares, dashed line, n = 9) where sensitivity improved at several frequencies and was stable through N10 (open squares, solid line, n = 13). Wild-type controls (inverted black triangles, n = 30) were not statistically different by generation and are grouped for clarity. See Supplemental Table 1 for statistical analysis. Error bars represent SEM.

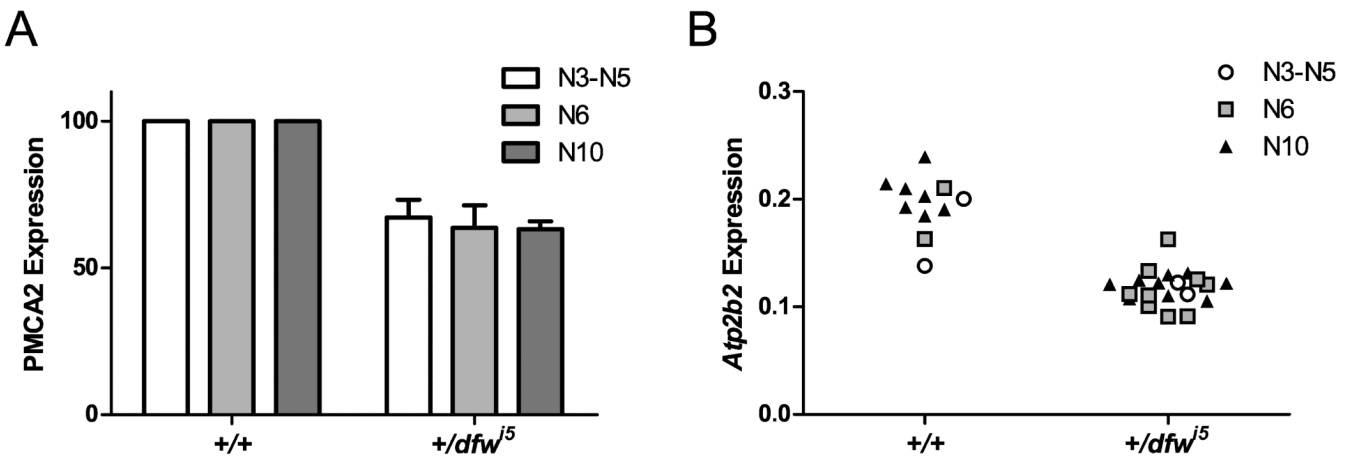

Fig. 6.

Protein and RNA expression levels in +/*dfw*^{j5} brainstem are not affected by generation. (A) PMCA2 was quantified from several Western blots of +/*dfw*^{j5} animals and generation-matched controls. Heterozygote expression is represented as a percentage of wild-type for generational groups N3-N5 (open bars, n = 3 blots), N6 (light gray bars, n = 5 blots) and N10 (dark gray bars, n = 6 blots). There is no statistical difference between generations in a two-way ANOVA. Error bars represent SEM. (B) Total *Atp2b2* is reduced in heterozygotes (+/*dfw*^{j5}) compared to wild-type (+/+) mice with no differences in absolute expression level across generational groups in a two-way ANOVA. A total of 11 samples from control mice were split into three generation groups: N3-N5 (open circles, n = 2), N6 (gray squares, n = 2) and N10 (black triangles, n = 7). A total of 20 +/*dfw*^{j5} samples were quantified and split into three generation groups: N3-N5 (open circles, n = 2), N6 (gray squares, n = 9) and N10 (black triangles, n = 9).